Nuclear Instruments and Methods in Physics Research A 454 (2000) 130–135

NUCLEAR INSTRUMENTS & METHODS IN PHYSICS RESEARCH Section A

www.elsevier.nl/locate/nima

Digital mammography with multi-electrode ionization chamber

V.R. Groshev, V.R. Kozak, V.I. Nifontov, S.M. Pishenuok, A.A. Samsonov, L.I. Shekhtman*, V.I. Telnov

Budker Institute for Nuclear Physics, 630090 Novosibirsk, Russia

Abstract

For viewing micro-calcifications smaller than 100 μm investigation of image formation in mammography shows that a significant dose to the patient is imperative. We propose a novel one-dimensional Multi-electrode Ionisation Chamber (MIC), with high spatial resolution, and lowered doses. In this work, first results from a prototype are presented. High spatial resolution is demonstrated working with Xe mixture at high pressure. An addition of a Gas Electron Multiplier (GEM) allowed an improvement in sensitivity up to almost single-photon level. © 2000 Elsevier Science B.V. All rights reserved.

1. Introduction

Radiography of mamma gland (mammography) is still one of the most often used examinations for diagnostics. In order to see some limitations of this method we consider basic features of image formation in mammography.

The mamma gland is compressed down to ~ 5 cm thickness. It is combined of soft tissues with some fibre-like and node-like structures, with size down to 1 mm and contrast in 20 keV X-rays down to ~ 1%. The most difficult objects to view are micro-calcifications that are composed of $Ca_5(PO_4)_3OH$ with the size down to 0.1 mm and less. If we assume no intrinsic noise in the detector, the noise at the image will be proportional to the square root of X-ray flux passing through the object. In Fig. 1 the image signal-to-noise ratio is shown as a function of X-ray energy. Here, we took the contrast of micro-calcification inside 4, 5 and 6 cm of soft tissue as a signal and the square root of flux after the object, as noise. From the figure we can see that the optimal energy to view such an object is ~ 20 keV. In Fig. 2 a contrast of 0.1 mm size calcification introduced into 5 cm of soft tissue (1–1 mixture of muscle and fat) is shown as a function of X-ray energy. The contrast at 20 keV is equal to ~ 10%. If a pixel size is less than 100 μm, in order to view the object, pixel noise has to be less than the contrast by a certain factor [1]. It means that the detector has to accumulate several hundred photons per pixel in this region.

Following the simple assumption about quantum-limited noise at the image, one can find that in order to view a micro-calcification, the flux at the surface of an object has to be reversed proportional to the size of micro-calcification to the power 4 (see

* Corresponding author.
E-mail address: lshekhtm@inp.nsk.su (L.I. Shekhtman).

PII: S0168-9002(00)00814-7

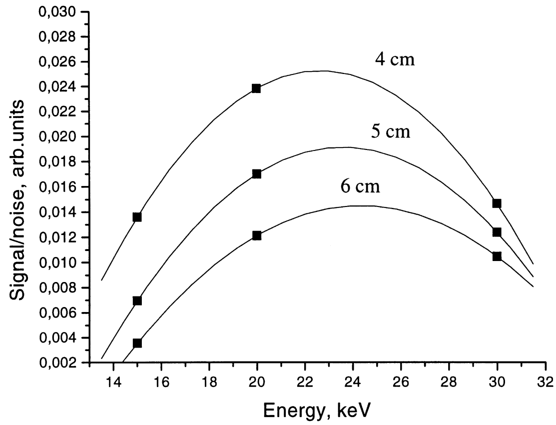

Fig. 1. Signal-to-noise ratio versus X-ray energy for different thickness of the object.

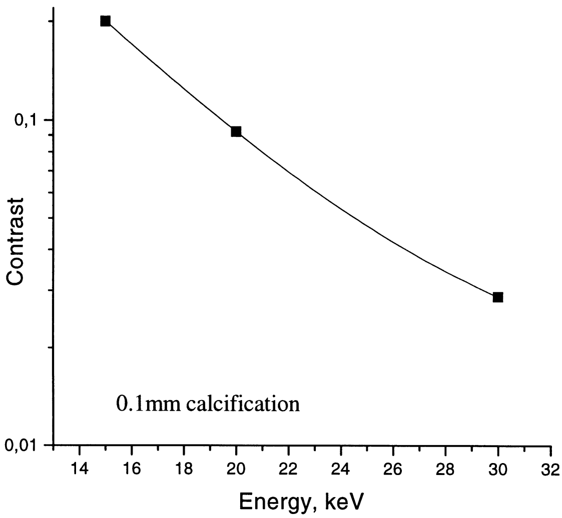

Fig. 2. Image contrast of 0.1 mm calcification in 5 cm thick soft tissue as a function of X-ray energy.

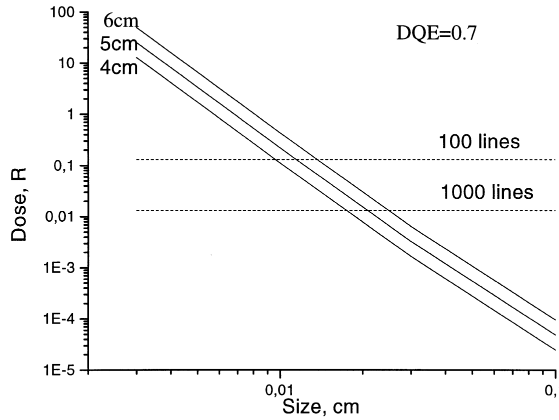

Fig. 3. Dose needed to view a micro-calcification as a function of size of this micro-calcification.

Appendix A). In Fig. 3 we show the result of calculations of the object surface dose which is necessary to view a micro-calcification as a function of the size of this micro-calcification. From the figure we can see that in order to view a micro-calcification below 0.1 mm the surface dose has to be comparable or higher than 1 R ($\sim$ 0.01 Gy).

Limitation on the dose level becomes even stronger if a one-dimensional detector is used in scanning mode. In this case the tube load becomes higher than in case of a true two-dimensional detector by a factor that is equal to the ratio of total exposure time over exposure time of one line. This number represents the number of lines in an image. Assuming that we can get a mammography tube with a maximum load capacity of 600 mAs [2] and using data from Ref. [3] to convert tube load into the dose at a distance of 50 cm, we get the maximum dose that can be delivered to the surface of an object is $\sim$ 10 mR (1000 lines in the image). This limit is marked with a dashed line in Fig. 3. From the figure we see that in this case, a minimum size of calcification which can be viewed is about 0.2 mm (for 5 cm thick soft tissue).

In this paper we propose to build a detector for digital mammography based on one-dimensional multi-electrode ionisation chamber (MIC). The chamber works without any amplification or with small amplification ($\sim$ 10) provided with Gas Electron Multiplier (GEM). The first results obtained with the prototype of such detector are presented.

2. Detector description and results from the prototype

Ionisation chambers have been used for X-ray imaging in angiography with synchrotron radiation [4] and for whole-body radiography [5]. This detector is simple in construction, robust and can provide necessary efficiency, rate capability and spatial resolution.

We have designed a multi-electrode ionisation chamber for mammography that consists of a multi-strip plane made on printed circuit board (PCB) together with the front-end electronics. The strips are directed to the source of radiation placed at a distance of 50 cm. The pitch of the structure at the wide side is 125 μm. Each strip is connected to the input of integrator array chip RL0128MB produced by EG&G Reticon [6]. The integrator chip contains 128 channels of low-noise integrators with analog buffer and multiplexer. The output of each chip is connected to ADC which converts signals to digital form synchronously with the readout of the chip. Information from the output of ADC is stored in 128-word buffer. Complete detector contains 12 cells with integrator chip, ADC and memory buffer. The total number of channels is 1536. All memory buffers will be read out through Ethernet link to Pentium PC. The PCB with electronics and multi-strip structure is put into a cylindrical high-pressure box made of aluminium alloy with the entrance window of 1 mm thick carbon fibre. High-voltage electrode that pushes ionisation down to the multi-strip structure is placed 2 mm above the PCB (Fig. 4).

Tests of the front-end electronics and main parameters of the detector have been performed. The prototype consists of a multi-strip structure with 200 μm pitch bonded to 64-channel version of the integrator chip with its output connected to the electronic cell described above. The high-pressure box with the PCB and drift electrode has been filled with Xe–CO_2 (80–20) gas mixture up to 5 atm. An X-ray tube with Mo anode has been used with maximum intensity at 18 keV.

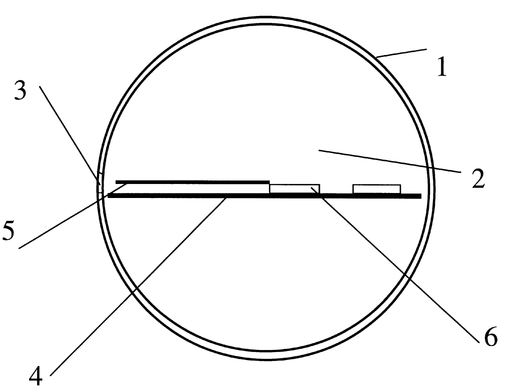

Fig. 4. Cross-section of the MIC for mammography. 1 – Aluminium high-pressure box; 2 – gas volume; 3 – carbon fibre inlet window; 4 – PC board with multi-strip structure; 5 – drift electrode; 6 – read-out electronics.

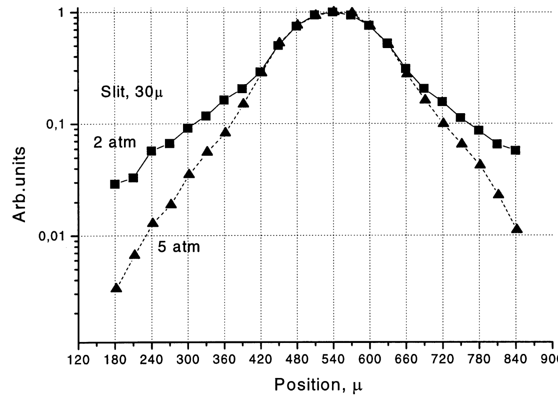

Fig. 5. Channel response function of the MIC prototype for 2 and 5 atm of Xe + CO_2 gas mixture.

Spatial resolution of the prototype has been tested with the help of a 30 μm slit. The chamber was irradiated through the slit and channel response has been measured as a function of slit position. The result of the measurement is shown in Fig. 5 for 2 and 5 atm. Channel response curve for 2 atm has a halo that is suppressed at 5 atm. This halo is caused by higher-energy photoelectrons with long range.

Detective quantum efficiency (DQE) has been measured as a function of photon flux through a single channel. Exposure time was tuned to 3 ms. The detector performed 100 exposures and readout cycles. RMS of the signal in each channel was calculated as well as the average value of the signal. Input flux was calculated according to the calibration of X-ray tube current performed before. According to the definition

$$\mathrm{DQE} = (s/n)^2_{\mathrm{out}}/(s/n)^2_{\mathrm{in}} \quad (1)$$

where the notation s/n means signal-to-noise ratio. If N_n is the number of photons equal to noise rms

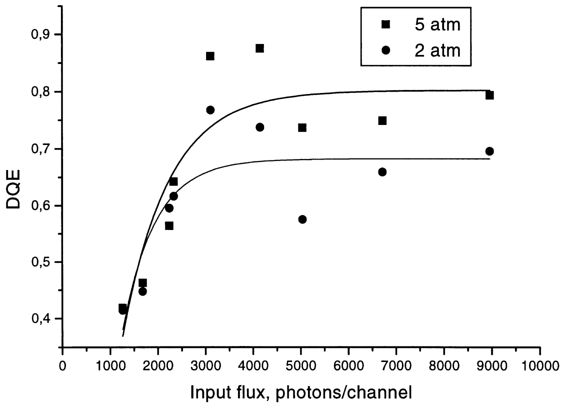

Fig. 6. DQE as a function of photon flux per channel for two different pressures of the gas mixture.

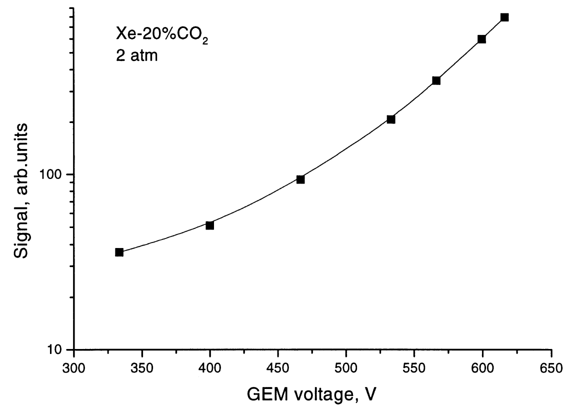

Fig. 7. Signal as a function of GEM voltage.

of a single channel and ε is the fraction of input flux absorbed in the sensitive volume, then

$$\mathrm{DQE} = \varepsilon/(1 + N_{\mathrm{n}}^2/\varepsilon N). \tag{2}$$

Here, N is average input photon flux through a single channel within exposure time. From Eq. (2) we can see that at high flux DQE is constant and equal to ε, and at low flux it drops due to the intrinsic noise of the detector. Results of the measurements are shown in Fig. 6 for 2 and 5 atm. The values of DQE at high flux agree very well with the calculation of the absorption of 18 keV X-rays in 30 mm layer of gas mixture with 3 mm dead zone. However, the DQE drops at around 1600 photons per channel that corresponds to ~ 40 photons noise rms. According to the specifications of the integrator chip its noise is equal to 1500 electrons or approximately to two 18 keV photons. The chip does not contain any amplifier at the output of the multiplexer. Signal from one 18 keV photon give at the output (15 pF feedback capacitor) $\sim 7\,\mu\mathrm{V}$. One bin of 14-bit ADC with 5 V range corresponds to $\sim 300\,\mu\mathrm{V}$. Hence, 1 ADC bin is equal to about 40 photons and therefore the ADC noise determines total noise of electronic chain rather than the integrator noise.

In order to solve this problem and improve DQE we had to introduce some amplification either to the electronic chain or into the detector itself. The Gas Electron Multiplier (GEM) was used to introduce uniform gas amplification between the conversion region and multi-strip structure. GEM is made from thin kapton foil double clad with copper. Narrow holes are etched through the material. Gas amplification starts in the holes when high voltage is applied between two sides of the structure. Detailed description of GEM and its properties can be found in Ref. [7]. The possibility of GEM operation at high pressure was studied in Ref. [8].

A 50 μm thick GEM with 80 μm and 140 μm diameter and pitch of holes respectively has been inserted 1 mm above the multi-strip plane. Performance of the detector with GEM was tested at 2 atm. In Fig. 7 the dependence of signal versus GEM voltage is shown. Amplification of more than 30 can be reached before the structure started to discharge. This amplification allowed improvement of the sensitivity to almost single photon per ADC bin. GEM amplification has improved the DQE at lower fluxes that can be observed in Fig. 8. Here we can see the comparison of DQE versus flux performance with and without GEM. With GEM, DQE is stable in the range between 300 and 6000 photons/channel. In case without GEM, DQE was dropping at ~ 2000 photons/channel already. Lower value of DQE with GEM can be explained by some misalignment of the foil that partly shadowed the beam. There is some drop of DQE at higher rates that can be explained by limited rate capability of GEM (note that 10 000 photons per

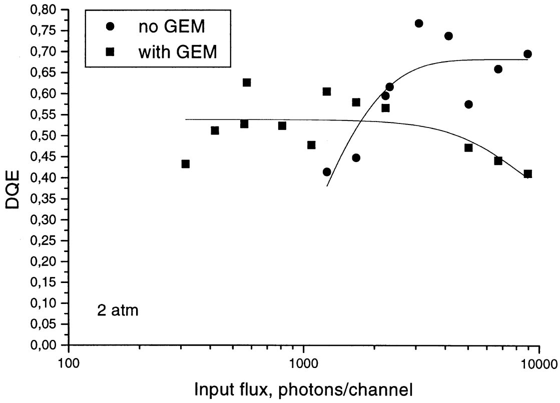

Fig. 8. DQE as a function of flux per channel with GEM amplification and without it.

channel corresponds to $\sim 10^7\,\mathrm{mm}^{-2}\,\mathrm{s}^{-1}$ flux density).

3. Conclusions

A simple analysis of image formation in mammography shows that micro-calcifications smaller than 100 μm cannot be viewed without significant dose delivered to a patient. We also showed that a scanning technique is possible with one-dimensional position sensitive detector and a powerful enough X-ray tube.

A prototype of the one-dimensional Multi-electrode Ionisation Chamber (MIC) was tested, with the proposed electronic chain and low-noise integrator array chip. High spatial resolution with 5 atm Xe mixture was demonstrated. However, the DQE dropped at rather high X-ray flux, explained by the low sensitivity of the electronic chain.

Additional amplification has been introduced with Gas Electron Multiplier that has provided multiplication of ~ 30 at 2 atm. The DQE measured with GEM has been stable down to ~ 100 photons/channel.

Stable performance of the detector with GEM still has to be tested at higher pressures. We plan that the final system will include amplification stages in the electronic chain that will allow to use GEM at higher pressures with lower multiplication.

Appendix A. Calculation of the surface dose necessary to view a micro-calcification

We will define the following notations used in the equations below.

- J_0 flux density at the surface of the object
- J flux density after the object with calcification
- ΔJ difference between flux density after the object without calcification and with calcification
- L thickness of the object
- a size of calcification (with cubic shape)
- μ linear absorption coefficient in a calcification;
- μ_0 linear absorption coefficient of the tissue around calcification.

Flux behind the object with calcification is equal to

$$J = J_0\ \exp[-(L-\mathrm{a})\mu_0 - a\mu] \sim J_0\ \exp[-\mu_0 L](1 - a\Delta\mu). \tag{A.1}$$

The difference between the flux behind the object with calcification and without is approximately equal to

$$\Delta J \sim J_0\ \exp[-\mu_0 L] - J_0\ \exp[-\mu_0 L](1 - a\Delta\mu) = J_0 a\Delta\mu\ \exp[-\mu_0 L]. \tag{A.2}$$

Total flux through the calcification is

$$\Delta N \sim J_0 a^3 \Delta\mu\ \exp[-\mu_0 L]. \tag{A.3}$$

In order to see the difference between the flux behind calcification and behind soft tissue, the difference between the total flux through the calcification and through the similar region nearby has to be larger than noise rms by a certain factor [1]. This factor is different for different observer but normally it is about or larger than 5. Thus

$$\Delta N/\sqrt{N} = 5 \tag{A.4}$$

where N is total flux through the region of background area equal to the calcification in size. From Eqs. (A.1) and (A.2) we obtain

$$\Delta\mu a^2 \sqrt{J_0\ \exp[-\mu_0 L]} \sim 5 \tag{A.5}$$

or

$$J_0 = 25(\Delta\mu)^{-2} a^{-4}\ \exp[\mu_0 L]. \tag{A.6}$$

If factor K_D is the conversion between the flux density and dose, then the surface dose is equal to

$$D = K_D 25(\Delta\mu)^{-2} a^{-4} \exp[\mu_0 L]. \quad (A.7)$$

References

[1] A. Martinez-Davalos, R.D. Speller, J.A. Horrocks, D.J. Miller, S.E. Baru, A.G. Khabakhpashev, O.A. Ponomarev, L.I. Shekhtman, Phys. Med. Biol. 38 (1993) 1419.

[2] Phillips Medical Systems, private communications.

[3] V.V. Kljuev (Ed.), Pentgenotekhnika, Mashinostroenie, Moscow, 1980.

[4] H.J. Besch, Nucl. Instr. and Meth. A 360 (1995) 277.

[5] E.A. Babichev et al., Nucl. Instr. and Meth. A 419 (1998) 290.

[6] EG&G Reticon, MB Series, Amplifier–Multiplexer array chips, 055-0343, January 1997.

[7] F. Sauli, Nucl. Instr. and Meth. A 386 (1997) 531.

[8] A. Bondar et al., Nucl. Instr. and Meth. A 419 (1998) 418.